

1 Stem-like CD8+ T cells preserve HBV-specific responses in HBV/HIV co-infection

2 Jay Preechanukul¹, Aljawharah Alrubayyi², Bo Sun³, Edward Arbe-Barnes¹, Jonida Kokici¹, Frances
3 Gorou¹, Sarun Prasitdumrong¹, Kelly A.S. da Costa¹, Natasha Fisher-Pearson², Noshin Hussain¹,
4 Stephanie Kucykowicz¹, Indrajit Ghosh⁴, Fiona Burns^{5,6}, Sabine Kinloch⁵, Pedro Simoes⁵, Sanjay
5 Bhagani^{1,7}, Patrick T F Kennedy⁸, Mala K Maini¹, Rachael Bashford-Rogers⁹, Upkar S Gill⁸, Dimitra
6 Peppas^{1,4,5}

7 ¹Division of Infection and Immunity, University College London, London, UK

8 ²Nuffield Department of Clinical Neurosciences, University of Oxford, UK

9 ³Nuffield Department of Clinical Medicine, University of Oxford, UK

10 ⁴Mortimer Market Centre, Department of HIV, CNWL NHS Trust, London, UK

11 ⁵The Ian Charleson Day Centre, Royal Free Hospital NHS Foundation Trust, UK

12 ⁶Institute for Global Health, University College London, UK

13 ⁷Department of HIV Medicine, Royal Free Hospital NHS Foundation Trust, UK

14 ⁸Barts Liver Centre, Barts & The London School of Medicine & Dentistry, QMUL, UK

15 ⁹Department of Biochemistry, University of Oxford, UK

16

17 Abstract

18 **Objective:** Chronic HBV infection disproportionately affects people living with HIV, who are often
19 excluded from functional cure studies. This study investigates CD8⁺ T cell profiles in HBV mono-
20 infection versus HBV/HIV co-infection, examining the impact of long-term therapy on virus-specific
21 responses with the goal of informing therapeutic strategies for immune restoration.

22 **Design:** We analysed CD8⁺ T cell responses in 61 participants (HBV n=20, HBV/HIV n=20, HIV
23 n=21), on suppressive antiviral therapy. We assessed transcriptomic and proteomic profiles, focusing
24 on exhaustion markers alongside virus-specific functional capabilities.

25 **Results:** Transcriptomic analysis revealed a distinct signature in co-infection, with upregulation of
26 genes associated with TCR signaling, inhibitory pathways and progenitor-exhausted markers (*XCL2*,
27 *TCF7*, *PDCD1*, *IL7R*). This gene profile scored highly for a precursor exhausted (Tpex) CD8⁺ T cell
28 signature, reflecting a "stemness" programme that maintains plasticity despite chronic antigen
29 exposure. Proteomic analysis confirmed higher frequencies of precursor exhausted TCF-
30 1⁺CD127⁺PD-1⁺ CD8⁺ T cells in co-infection, while HBV mono-infection showed predominance of
31 terminally exhausted Tox^{high}TCF-1⁺CD127⁺ cells. These differences correlated with more robust,
32 polyfunctional HBV-specific responses in co-infection against surface and core antigens. Lower
33 HBsAg levels and longer treatment duration in co-infection associated positively with Tpex
34 populations and functional responses and inversely with terminal exhaustion.

Conclusion: Our findings demonstrate that individuals with well-controlled HBV/HIV co-infection maintain more robust CD8⁺ T cell responses with preserved stem-like properties supporting ongoing antiviral function. These results underscore the benefits of early antiretroviral intervention and the need for tailored immune-modulatory therapies to restore antiviral functionality in these diverse patient populations.

40

WHAT IS ALREADY KNOWN ON THIS TOPIC

- Chronic hepatitis B virus (HBV) infection is marked by a progressive dysfunction of CD8⁺ T cells, which are crucial for antiviral responses. Traditionally these responses were thought to be more severely impacted in people with HBV/HIV co-infection.

WHAT THIS STUDY ADDS

- Our study provides new insights into the heterogeneous functional profiles of HBV-specific CD8⁺ T cells in people with HBV and HBV/HIV co-infection in the current antiretroviral therapy (ART) era.
- People living with HBV/HIV co-infection suppressed on antivirals have a higher prevalence of precursor exhausted CD8⁺ T cells (Tpex), alongside more effective antiviral responses when compared to those with HBV mono-infection.
- Our data demonstrate intrinsic differences in T cell profiles, revealing a paradoxical increase in terminally exhausted CD8⁺ T cells in people with HBV mono-infection.

HOW THIS STUDY MIGHT AFFECT RESEARCH, PRACTICE OR POLICY

- By providing a clearer understanding of CD8⁺ T cell dynamics in HBV mono-infection and HBV/HIV co-infection, our findings could inform the design of tailored immunotherapies aimed at revitalising antiviral responses.
- Furthermore, this research may influence practices regarding clinical management emphasising the need for early intervention strategies and individualised approaches tailored to T cell profiles rather than solely based on infection status.

61
62
63
64
65
66
67
68
69
70
71
72
73
74
75
76

77 INTRODUCTION

78 Chronic hepatitis B (HBV) infection remains a significant health challenge, particularly among people
79 living with HIV (PLWH), where approximately 10% are affected by concurrent chronic HBV¹. Yet
80 people with co-infection are traditionally excluded from clinical trials, and their immune
81 responses/HBV-specific immunity remain critically under-investigated, especially in the era of potent
82 HBV-active antiretroviral therapies (Tenofovir Disoproxil Fumarate (TDF)/Tenofovir Alafenamide
83 (TAF). These responses are important to elucidate in order to develop new and safe
84 immunotherapeutic strategies and guide their involvement in the HBV-cure agenda.

85 The pathogenesis of chronic HBV infection is influenced by immune responses, particularly those
86 mediated by CD8⁺ T cells, which are instrumental for viral control, and are thus promising targets for
87 immunotherapeutic approaches aimed at achieving a functional cure (FC) [HBsAg loss] for chronic
88 HBV (cHBV) infection². cHBV results in diminished CD8⁺ T cell responses characterised by variable
89 degrees of functional impairment, including upregulation of inhibitory molecules, specific
90 transcriptional profiles and metabolic dysfunction, collectively reflecting a state of exhaustion due to
91 prolonged antigen persistence³⁻⁸. HIV co-infection is thought to exacerbate these functional deficits,
92 leading to more pronounced dysregulation of HBV-specific CD8⁺ T cell responses due to the
93 combined influence of HIV and HBV⁹. In early studies, people with untreated co-infection had
94 substantially fewer and narrower responses to HBV peptide stimulation compared to those with HBV
95 mono-infection¹⁰. Although limited research examining responses to antiviral therapy prior to the
96 introduction of highly active antiretroviral therapy (HAART) indicated a modest recovery of HBV
97 immune responses, these responses remained suboptimal¹¹. Notably, people with co-infection are
98 more likely to achieve a FC following the introduction of ART^{12 13}; however, the effects of long-term
99 viral suppression on reconstitution of HBV-specific responses remain unknown. Our recent findings
100 have indicated that, in the context of long-term therapy, people with HBV/HIV co-infection exhibit more
101 favourable immunological profiles, evidenced by better preserved natural killer (NK) cell responses
102 and lower levels of HBsAg and peripheral surrogates of HBV activity compared to those with HBV
103 mono-infection¹⁴. Given the critical role of CD8⁺ T cells in HBV control, there is an urgent need for
104 increased insights into the specific profiles of CD8⁺ T cells in people with HBV/HIV.

105 Recent studies have revealed that exhausted CD8⁺ T cell populations are not homogeneous; they
106 exhibit developmental and functional diversity, including the presence of stem-like progenitors
107 expressing T cell factor 1 (TCF-1)¹⁵. These progenitors or precursors of exhausted CD8⁺ T cells
108 (Tpex) retain the potential to mount effective immune responses¹⁶, allowing for the possibility of
109 therapeutic intervention aimed at restoring immune efficacy¹⁷.

110 Importantly, the nature of T cell dysfunction in cHBV may differ from other chronic infections.
111 Emerging evidence suggests that T cell dysfunction in cHBV infection incorporates traits more
112 reminiscent of a state of tolerance or anergy¹⁸, underscoring the need for a more nuanced
113 understanding of these dynamics, particularly in the under-explored context of co-infection.

Understanding the heterogeneity of HBV-specific CD8⁺ T cells in various populations is therefore an important step for identifying potential targets for immunotherapy and uncovering novel molecular pathways that could enhance antiviral immune responses.

In this study, we aimed to address these critical gaps in understanding the immune responses of individuals with HBV/HIV co-infection compared to those with HBV mono-infection in the current ART era. We hypothesised that earlier initiation and long-term viral suppression with potent antiretroviral therapy might preserve functional CD8⁺ T cell responses in co-infection, contrary to traditional expectations of more severe immune dysfunction. We performed a detailed analysis at the single-cell level, complemented by assessments of functional virus-specific responses, to enhance our knowledge of the immunological landscape in these patient populations.

MATERIALS AND METHODS

Patient populations

A total of n=20 patients with HBV/HIV, n=20 people with HBV and n=21 with HIV were recruited at Mortimer Market Centre for Sexual Health and HIV research, the Ian Charleson Day Centre at the Royal Free Hospital (London, UK) or The Royal London Hospital (London, UK) following written informed consent as part of a study approved by the local ethics committee (Berkshire (REC 16/SC/0265) and London Bridge (REC 17/LO/0266) and conformed to the Helsinki declaration principles. All participants were negative for HCV infection and confirmed HCMV seropositive. PBMCs, plasma and serum were collected as part of this study. Additional demographic and clinical information can be found in **supplementary table 1**.

Single cell Sequencing

Library preparation and sequencing

PBMCs with >96% viability were used¹⁴. Library construction was performed using the 10x next GEM Chips Chromium single cell library 5' construction kit (10x Genomics, Pleasanton) as per the manufacturer's protocol. Briefly, a maximum of 3000 cells were combined with barcoded single cell VDJ gel beads, cells and partitioning oil onto Chromium Next GEM Chip K. The resulting 10x Barcoded, full-length cDNA was recovered and amplified overnight via PCR with primers against common 5' and 3' ends added during the GEM reverse transcription process. Resulting cDNA was purified using SPRIselect beads (Beckman Coulter, High Wycombe, UK). The amount and quality of cDNA was determined using TapeStation (Agilent, UK). Purified libraries were analyzed by Novogene. Donor characteristics analysed by single-cell RNAseq data are described in **supplementary table 2**.

Single-Cell RNA Sequencing Preprocessing and Procedures

Single-cell RNA sequencing (scRNA-seq) preprocessing and downstream analyses for this study have been previously described in detail¹⁴. Briefly, we excluded any cell barcodes with fewer than 200 detected transcripts or more than 10% mitochondrial-encoded genes, retaining only cells expressing

fewer than 3000 genes. We considered genes if they were expressed in at least five cells. After confirming that our data and the Azimuth PBMC reference atlas¹⁹ showed similar distributions of transcripts and gene counts, we demultiplexed hash-tagged samples using the Scanpy external implementation of Hashsolo²⁰ and excluded doublets using Solo. For dataset integration, raw counts from the top 3000 highly variable genes were used to train a scVI model, which generated 20 latent dimensions for embedding. We then computed a nearest neighbor graph on these dimensions for cell clustering via iterative Leiden clustering at increasing resolutions to capture both coarse and fine cell type heterogeneity. Automated cell type annotations were performed with Cell typist²¹, followed by manual validation based on marker gene expression and hierarchical clustering.

Differential gene expression was calculated with Seurat's FindMarkers function (using DESeq2 as the statistical backend), controlling for variable sample sizes across study groups. Functional enrichment analysis was carried out using the XGR package for pathway-level assessment and GSEApy for gene set enrichment analysis²². Differential abundance analysis was performed with the R implementation of Milo²³. For the Milo buildGraph function, k was set to 40, and all 128 dimensions of the DRVI latent embedding were used. Where described, gene set scores were calculated with Scanpy's score_genes function. The Tpx-score genes were derived from Zheng et al.²⁴. For the unbiased gene program discovery analysis, DRVI was implemented with default parameters²⁵.

Ex-vivo phenotypic analysis of CD8⁺ T cells

The fluorochrome-conjugated antibodies utilised are detailed in **supplementary table 3**. Briefly, cryopreserved PBMCs were thawed and allowed to rest at 37 °C in a complete RPMI medium (Penicillin-Streptomycin, L-Glutamine, HEPES, non-essential amino acids, 2-Mercaptoethanol, and 10% Fetal Bovine Serum (FBS)). The cells were washed, resuspended in PBS, and incubated for 20 minutes at 4°C with various antibody combinations along with a fixable live/dead stain (Invitrogen). The cells were subsequently fixed and permeabilised to facilitate the detection of intracellular antigens. For the identification of intranuclear markers, the Foxp3 intranuclear staining buffer kit (eBioscience) was used according to the manufacturer's protocol. Total PBMCs were stained with APC-labeled HBV (core 18-27, envelope 183–191, envelope 335–343, and envelope 348–357), HCMV (pp65 495-504), and HIV (Gag 77-86) dextramers (Immudex) at 37°C for 15 minutes in complete RPMI with 10% FBS. After pelleting, cells were further stained as above. Dextramer staining was deemed positive if a distinct population (>0.02%) was identified. Data acquisition was conducted on a BD Fortessa X20 via BD FACSDiva8.0 (BD Bioscience), and the resulting data analysis was carried out using FlowJo 10 (TreeStar). The gating strategy for identifying CD8⁺ T cells is illustrated in **supplementary figure 2A**. Stochastic neighbor embedding (SNE) analysis was performed on the MRC Cytobank platform to visualise high-dimensional data.

Functional assessment of virus-specific CD8⁺ T cells

Intracellular cytokine staining (ICS) was performed as previously described²⁶. PBMCs were thawed and allowed to rest at 37 °C in complete RPMI medium with 5% CO₂. PBMCs were then stimulated for 12-16 hours using 3 µg/mL of overlapping peptide pools from HBV (large envelope and capsid), HIV-1 Gag, or positive control peptide pools derived from cytomegalovirus (HCMV), Epstein Barr virus (EBV) and influenza virus (CEF pool) (**supplementary table 4**), alongside 0.005% DMSO as a negative control. This was done in the presence of αCD28/αCD49d co-stimulatory antibodies (1 µg/ml), Brefeldin A (eBioscience). Post-stimulation, cells were stained with anti-CCR7 at 37 °C for 30 minutes, then surface stained at 4 °C for 20 minutes along with a live/dead stain. Following fixation and permeabilisation, intracellular cytokines (IFN-γ APC, CD154 PE-Cy7, TNF-α FITC, IL-2 PerCP-eFluor 710) were assessed. Data acquisition was performed using a BD Fortessa X20, and analysis was conducted using FlowJo 10. Virus-specific CD8⁺ T cells were identified as those expressing combinations of IFN-γ, TNF-α, IL-2. A detailed list of antibodies used is found in **supplementary table 3**.

Statistical methods

Prism 9 (Graphpad, San Diego) and R (URL <https://www.R-project.org/>) was used for statistical analysis. The Mann–Whitney U-test was used for single comparisons of groups, and the Wilcoxon-paired t-test was used to compare two paired groups. Correlation analysis was carried out with non-parametric Spearman correlation. Kruskal Wallis testing followed by Dunn test was used for pairwise comparison between gene module scores. The statistical significance is indicated in the figures. (* $p < 0.05$, ** $p < 0.01$, *** $p < 0.001$, and **** $p < 0.0001$).

RESULTS

Single cell analysis of CD8⁺ T cells shows reduced cytotoxicity gene expression and enriched TCR signalling pathways in HBV/HIV co-infection

To explore the effects of HBV and combined effect of HBV/HIV on CD8⁺ T cell populations, we utilised available single-cell sequencing PBMC data (using 10X Chromium (5' transcriptome) from $n = 5$ HBV/HIV and $n = 6$ HBV donors, predominately on TDF treatment (**supplementary table 2**)¹⁴. To account for the effect of human cytomegalovirus (HCMV), all donors were confirmed human HCMV-seropositive. CD8⁺ T cell subsets – naive CD8⁺ T cell (TN), central memory (TCM) CD8⁺ T cell, effector memory (TEM) CD8⁺ T cell, terminally differentiated effector memory (TEMRA) CD8⁺ T cell and memory precursor effector cell (MPECS), were identified by clustering based on their differentially expressed genes (DEGs) and visualised on a uniform manifold approximation and projection (UMAP) (**figure 1A-B**).

To gain insight into cellular differential abundance and compositional shifts between HBV mono-infection vs. HBV/HIV co-infection, MiloR was used for differential abundance testing. While naive CD8⁺ T-cells trended towards more abundance in HBV mono-infection, we found that most of the significant changes driven by HBV/HIV co-infection were within the CD8⁺ TEM compartment (**figure**

1C). Comparing the transcriptional profiles of CD8⁺ TEM cells between patient groups, donors with co-infection showed an up-regulation of *KLF10*, which encodes an effector protein of transforming growth factor beta (TGF- β) signaling²⁷, *DDX3Y*, which is involved in RNA binding and the formation of intramolecular interactions, and *WHAMM*, which encodes a protein that mediates membrane dynamics and cytoskeletal organisation within cells²⁸ (**figure 1D**). In contrast, several cytotoxicity genes were upregulated in the CD8⁺ TEM and TEMRA clusters of mono-infected patients (**figure 1D**), correlating with higher cytotoxicity scores observed in these populations in HBV mono-infection (**supplementary figure 1A**). Genes driving CD8⁺ T cell remodeling were reflected in differentially regulated gene pathways, with enrichment of TCR downstream signaling, co-stimulation, PD-1 signalling and TCA cycle and translation observed in the CD8⁺ T cell populations in the co-infection group (**figure 1E**).

Next, we sought to identify de novo gene programs that might be differentially used across mono-infection and co-infection. To do so, we used DRVI²⁵ (an unsupervised deep generative model that learns nonlinear, disentangled representations of single-cell omics data, allowing us to discover biologically meaningful latent dimensions and nonlinear gene programs. Applying DRVI led to the identification of 39 gene programs (**supplementary figure 1B–C**). Notably, “DR17” was differentially upregulated in the same neighborhood that MiloR analysis pinpointed as being enriched in HBV/HIV co-infection (**figure 1F–G**).

Among the relevant genes in DR17 were *CD160*, *TIGIT*, *XCL2*, *CHI3L2*, *EOMES*, *TOX*, *PDLIM1*, and *CMC1* (**figure 1H**). Upregulation of *CHI3L2* (involved in inflammation regulation)²⁹ and *CMC1* (involved in mitochondrial function)³⁰ suggest cellular and metabolic adaptations of CD8⁺ T cells in co-infection. Of particular interest, *XCL2* has been associated with progenitor or precursors of exhausted (Tpex) T cells³¹. Further interrogation showed that T_{pex} markers (*TCF7*, *PDCD1*, *IL7R*, *GZMK*, *TOX*) were present and *HAVCR2* (which encodes TIM-3, characterising terminally exhausted populations) was notably absent in this neighbourhood (**figure 1I**), consistent with a Tpex phenotype, associated with a favourable response to combination therapy in hepatocellular carcinoma³¹. In addition, co-expression of inhibitory receptors (*CD160*, *TIGIT*) and exhaustion-associated transcription factors (*EOMES*, *TOX*) supports a Tpex-like transcriptional signature in these cells^{17 32}. To validate whether this co-infection-enriched neighbourhood indeed displayed Tpex-like features, we calculated a Tpex score based on Tpex-associated genes identified through a pan-cancer single-cell atlas²⁴. As expected, this region scored highly for the Tpex signature alongside naïve and MPEC populations, likely reflecting a shared “stemness” gene programme that underlies both memory-precursor and stem-like exhausted states (**figure 1J**). Overall, these signatures suggest an adapted immune state in HBV/HIV co-infection where CD8⁺ T cells counter-balance inhibitory mechanisms with stemness features that could maintain plasticity and functional potential despite chronic antigen exposure.

Precursors of exhausted CD8⁺ T cells are enriched in HBV/HIV co-infection

To explore whether the proteomic profile of CD8⁺ T cells in individuals with HBV mono-infection (n = 20) and HBV/HIV co-infection (n = 20) mirrors transcriptomic signatures, we conducted a phenotypic analysis within our wider cohort. Matched donors with HIV mono-infection (n = 21) virally suppressed on antiretroviral therapy were utilised as a comparator group (**supplementary table 1**). Using a curated cytometry panel and gating strategy (**supplementary figure 2A**), we evaluated CD8⁺ T cell subsets. As expected, higher frequencies of CD8⁺ T cells were observed in the context of HIV infection (**supplementary figure 2B**). HBV/HIV co-infection and HIV mono-infection showed increased frequencies of CD8⁺ TEM and TEMRA, while HBV mono-infection predominantly exhibited CD8⁺ naive T cells, consistent with findings from single-cell analyses (**supplementary figure 2C-D**).

Using an unbiased global t-distributed stochastic neighbour embedding (t-SNE) high dimensional analysis and FlowSOM clustering, we further identified a distinct subpopulation (metacluster) that was more prominent in people with HBV/HIV co-infection relative to the other groups (**figure 2A**). This metacluster 1, which was more abundant in HBV/HIV co-infection, displayed a phenotypic signature characterised by the presence of CD45RA⁺CCR7⁺ TIM3⁺PD1⁺CD127^{high}TCF1⁺ (**figure 2A-B**). Manual gating analysis further confirmed increased frequencies of CD127^{high}TCF1⁺ CM/TEM CD8⁺ T cells, which were particularly expanded within specific donors with HBV/HIV co-infection (**figure 2B-C**), suggesting a less differentiated memory-like state with preserved stemness properties.

Building on the transcriptomic findings and FlowSOM clustering, we characterised the exhaustion landscape in greater detail across the study groups, with particular attention to co-expression patterns of TCF-1, CD127 and PD-1, signatures associated with Tpex versus terminal exhaustion (Tex) states on global CD8⁺ T cells (**figure 3A-C**). While conventional exhaustion/activation markers (PD-1, HLADR/CD38) showed no significant differences between groups (**supplementary figure 3A-B**), we observed reduced CD127 expression on CD8⁺ T cells in HBV mono-infection alongside elevated TOX levels (**supplementary figure 3C-D**), robust expression of which results in commitment to Tex³³. Higher frequencies of CD8⁺ T cells with a stem-cell Tpex phenotype expressing TCF-1⁺CD127⁺PD-1⁺ were identified in people with HBV/HIV compared to either mono-infection group (**figure 3B-C**), mirroring the transcriptomic enrichment of stemness-associated genes in this population. Conversely, Tex CD8⁺ T cells characterised by TCF-1⁻CD127⁻PD-1⁺ expression were predominant in HBV mono-infection (**figure 3B-C**). While TOX expression was similar across Tpex populations in all groups (**figure 3D**), TCF-1⁻CD127⁻PD-1⁺TOX⁺ cells were significantly increased in HBV mono-infection (**figure 3E**), in keeping with a terminal exhaustion state. Tpex cells resided primarily within the TEM compartment, while Tex cells were enriched in TEMRA populations in HBV mono-infection (**supplementary figure 4A-B**). To further address the differentiation stage of the particular CD127/TCF-1 subsets, we stained for the effector cell molecule granzyme-B. As expected, Tpex populations were further characterised by lower granzyme-B expression³⁴; by contrast granzyme-B⁺ Tex CD8⁺ T cells were predominant in HBV mono-infection (**supplementary figure 4C-D**) aligning with the higher cytotoxicity signatures observed in the transcriptomic data.

Collectively, our findings reveal distinct CD8⁺ T cell exhaustion landscapes in HBV versus HBV/HIV co-infection.

Higher frequency and polyfunctional HBV-specific CD8⁺ T cell responses in HBV/HIV co-infection compared to HBV

Having established distinct exhaustion profiles in global CD8⁺ T cell populations, we next sought to determine whether these phenotypic differences translated to functional discrepancies in virus-specific CD8⁺ T cell responses between individuals with HBV mono-infection and those with HBV/HIV co-infection. Intracellular cytokine staining (ICS) was employed to investigate the composition and polyfunctionality of T cell responses among individuals with HBV/HIV co-infection, as well as those with HBV and HIV mono-infection. PBMCs were stimulated overnight using overlapping peptides targeting the HBV surface (S) and core proteins, alongside CEF and HIV-1 gag peptides within the same individuals.

Notably, after overnight stimulation, higher magnitude HBV-specific responses, identified by co-expression of IFN- γ and TNF- α , were seen in donors with HBV/HIV co-infection relative to donors with HBV (**figure 4A-B**). Over 90% of donors with co-infection demonstrated detectable HBV-specific responses (>0.05% IFN- γ ⁺TNF- α ⁺ CD8⁺ T cells), compared to 50% in HBV mono-infection (**figure 4C**). Within individual donors, HBV-specific responses were comparable to those against CEF or HIV-1 gag peptides (**figure 4B**). HIV-1 gag-specific responses were similar between people with HBV/HIV co-infection and those with HIV mono-infection (**figure 4B**). HBV-specific CD8⁺ T cells displayed polyfunctional responses in people with co-infection, particularly against HBV surface protein (**figure 4D**). HBV-specific CD8⁺ T cells primarily displayed EM/TEMRA phenotypes, with core-specific responses in people with co-infection also exhibiting a more notable CM phenotype compared to HBV mono-infection (**Supplemental figure 5A-B**). While people with co-infection showed higher mean frequencies of CEF responses compared to those with mono-infection, these differences were not statistically significant and displayed similar polyfunctional profiles (**figure 4A, B and D**). Despite elevated PD-1 expression on both HBV- and HIV-specific CD8⁺ T cells compared to CEF-specific cells (**supplementary figure 5C-D**), this did not compromise their functional capacity, suggesting PD-1 expression in this context may not exclusively indicate exhaustion.

To further characterise HBV-specific CD8⁺ T cells, we employed MHC I dextramers to detect virus-specific CD8⁺ T cells directly *ex vivo* targeting known HLA-A*02-restricted epitopes. We focused on HBV_{env} (combined env_{183–191}, env_{335–343}, and env_{348–357}), pp65_{495–504} and Gag_{77–86} in a subset of HLA-A*02-positive donors with co-infection and detectable responses. We observed that HBV env-specific CD8⁺ T cells displayed higher frequencies of T_{pex} cells (PD-1⁺/CD127⁺) (**figure 5A**). Similar trends were observed for both HCMV pp65-specific and Gag-specific CD8⁺ T cells showing enrichment of CD127⁺PD-1⁺ (T_{pex} phenotype) compared to CD127⁺PD-1⁺ (T_{ex} phenotype) (**supplementary figure 6A, B**). Next, we assessed the expression of the transcription factor TCF-1 and anti-apoptotic molecule BCL-2 that have been shown to best determine the memory-like phenotype and cellular persistence of this subset³⁵. CD127⁺PD-1⁺ HBV env-specific CD8⁺ T cells contained higher mean

frequencies of TCF-1⁺ and BCL-2⁺ cells compared to CD127⁺PD-1⁺ populations (**figure 5B, C**), with HCMV-specific and HIV Gag-specific cells showing similar patterns(**supplementary figure 6C and D**). These results would be in keeping with the enhanced survival potential of this precursor exhausted subset.

HBsAg levels and treatment duration shape CD8⁺ T cell exhaustion profiles and functional responses

Having established distinct phenotypic and functional differences in CD8⁺ T cell responses between patient groups, we examined potential virological factors that might explain these immunological differences. Quantitative HBsAg analysis revealed significantly lower levels in people with HBV/HIV co-infection compared to those with HBV mono-infection (**figure 6A**), in keeping with our recent observations¹⁴. A greater percentage of people with HBV/HIV had HBsAg below 50 IU/mL, including some with levels below 1 IU/mL (**figure 6B**), potentially reflecting the longer duration of antiviral therapy in this group (average 14 years versus 4 years in mono-infection, **supplementary table 1**).

Correlation analyses revealed negative associations between circulating HBsAg levels and both functional HBV-specific responses and T_{pex} frequencies (**figure 6C**). Conversely, T_{pex} populations correlated positively with HBV-specific responses and treatment duration, while T_{ex} populations showed inverse relationships with functional responses, particularly against HBV core (**figure 6C**). Treatment duration also positively associated with HBV-specific responses, suggesting progressive immune restoration with sustained viral suppression. We did not detect any associations with age, CD4 count (including CD4 nadir) or CD4:CD8 ratio.

DISCUSSION

The goal of immune-based strategies for chronic HBV infection is to elicit functional and durable HBV-specific CD8⁺ T cell responses that can bolster antiviral control. Our findings challenge the conventional understanding of immune responses in HBV/HIV co-infection by demonstrating that individuals with well-controlled HBV/HIV co-infection on long-term suppressive therapy display enhanced preservation of functionally competent HBV-specific CD8⁺ T cells compared to those with HBV mono-infection.

The increased frequency of TCF-1⁺CD127⁺PD-1⁺ (T_{pex}) CD8⁺ T cells observed in people with co-infection aligns with emerging evidence demonstrating the critical role of these cells in maintaining antiviral responses during human chronic infection³⁶⁻⁴⁰. These memory-like CD8⁺ T cells, that occur early during infection^{41 42}, maintain proliferative capacity despite chronic antigen exposure and provide the proliferative burst following PD-1 pathway blockade^{16 17 31 34}. Our findings extend this concept to HBV/HIV co-infection, where we observe higher frequencies of T_{pex} cells and more robust HBV-specific responses than in HBV mono-infection. The preservation of a stem-like CD8⁺ T cell pool capable of sustained antiviral responses may facilitate HBsAg clearance in people with co-infection, who demonstrate higher rates of functional cure^{12 13}. Furthermore, these results align with our recent

work demonstrating enhanced NK cell ADCC in co-infection¹⁴, suggesting a better-preserved immunological profile favouring viral control.

The transcriptional signature of CD8⁺ T cells in HBV/HIV co-infection, suggests adaptive mechanisms allowing CD8⁺ T cells to navigate a potentially more complex immunological landscape due to the presence of two chronic viral infections. Upregulation of TCR signalling and inhibitory pathway genes (e.g., *CD160*, *TIGIT*, *PDCD1*) alongside genes involved in inflammation regulation (*CHI3L2*, *KLF10*) and mitochondrial function (*CMC1*) suggests a balanced immune response that prevents excessive inflammation while maintaining functional responses. Along these lines, PD-1 expression on Tpex virus-specific CD8⁺ T cells likely shields these populations from excessive TCR stimulation, preserving their stem-like properties¹⁵. This interpretation is supported by our observation that these populations maintain high expression of BCL-2 and TCF-1, markers associated with memory potential and cellular longevity, despite chronic antigenic stimulation³⁹. In contrast, HBV mono-infection exhibited a profile skewed toward terminal exhaustion, with elevated TOX expression, that transcriptionally/epigenetically programmes CD8⁺ T cell exhaustion³³, and linked to CD8⁺ T cell dysfunction during cHBV⁴³.

Our findings echo recent observations demonstrating that exhaustion profiles in global CD8⁺ T cells can predict functional capacity of HBV-specific responses⁶. The apparent paradox of better T cell functionality in co-infection could be explained by several factors. Significantly lower HBsAg levels observed in people with co-infection likely reduce antigen-driven exhaustion, supported by the negative correlation between HBsAg and functional T cell responses. This aligns with findings from previous studies demonstrating the detrimental effects of sustained HBsAg exposure on virus-specific T cells⁸. Earlier initiation of potent HBV-active therapy in people diagnosed with HIV leads to more rapid suppression of viral replication, as reflected by the longer average treatment duration in our co-infected cohort. This early intervention likely preserves the Tpex pool before terminal exhaustion occurs, consistent with our observation that treatment duration positively correlates with functional responses and Tpex frequencies. Additionally, the immunological milieu created by HIV infection⁴⁴ may modulate HBV-specific responses through altered cytokine profiles or reduced immune regulatory mechanisms. Our recent findings of enhanced proportions of adaptive/memory like NK cells in HBV/HIV co-infection¹⁴, with less inherent potential for excessive negative regulation of T cell responses^{45 46}, supports this broader immune remodelling hypothesis.

Multiple studies have demonstrated that targeting the PD-1 pathway can enhance HBV-specific CD8⁺ T cell function⁴⁷, and affect the HIV viral reservoir and virus-specific responses^{48 49}. Our data suggest that such approaches may be particularly effective in people with co-infection who maintain a higher proportion of Tpex cells. Similarly, approaches to target the TCF-1 pathway⁵⁰ and enhance stemness through IL-15 signalling⁵¹ or TOX manipulation even after Tex establishment⁵² could therefore provide therapeutic opportunities to rewire Tex cells in chronic infections.

Several limitations of our study warrant consideration. As a primarily cross-sectional investigation conducted on peripheral blood, we cannot directly extrapolate our findings to hepatic tissue. The observed differences may be significantly influenced by our cohort characteristics, particularly regarding infection routes and treatment histories, which may limit the generalisability of our findings. In Western settings, HBV/HIV co-infection typically occurs through sexual transmission in adulthood, while HBV mono-infection often results from vertical transmission, leading to fundamental differences in immune priming and tolerance. Additionally, our analysis focused on surface and core HBV-specific responses; extending this to other antigens would provide a more comprehensive understanding of virus-specific responses, as exhaustion profiles differ based on targeted antigens⁶³⁹.

Future longitudinal studies should examine how these immunological differences evolve over time in response to therapy and correlate with clinical outcomes. Tissue-based analyses would provide insight into the hepatic immune microenvironment, while functional studies examining the response of T_{pex} cells to immunotherapeutic interventions could inform personalised treatment approaches based on exhaustion phenotypes rather than infection status alone. Additional work beyond the scope of this study, will aim to provide more mechanistic insights into the maintenance of T_{pex} populations in co-infection that could identify novel targets for enhancing immune function.

Despite these limitations, our study provides the first evidence that in individuals with well-controlled HBV/HIV co-infection in the current ART era, CD8⁺ T cell responses are more robust and retain stem-like properties that support ongoing antiviral function. These findings underscore the benefits of early antiretroviral intervention and highlight TCF-1-expressing stem-like CD8⁺ T cells as a promising target for immunotherapeutic strategies aimed at achieving functional cure in chronic HBV infection.

Contributors

JP performed experiments, acquisition of data, analysis, and drafting of the manuscript; BS, AA, EAB, JK, FG, SP, KDC, NFP, NH, SK, performed experiments and contributed to data acquisition and analysis. IG, FB, SK, PS, SB, PTFK, MKM, RBS and USG contributed clinical samples, data interpretation and critical editing of the manuscript. DP contributed to the conception and design of the study, data interpretation, critical revision of the manuscript, and study supervision.

Funding

This work was supported by an NIH award (R01AI55182) and a UKRI Medical Research Council (MRC) Grant (MR/W020556/1) to D.P.; an Academy of Medical Sciences Starter Grant (SGL021/1030), Seedcorn funding Rosetrees/Stoneygate Trust (A2903) and Mid-Career Research Award from The Medical Research Foundation (MRF-044-0004-F-GILL-C0823) to U.S.G. B.S is supported by an NIHR Academic Clinical Lectureship (CL-2021-13-002).

Competing interests

The authors declare no competing interests.

Data availability statement

All data relevant to the study are included in the article or uploaded as online supplemental information.

Raw data for single cell sequencing reported in this study have been deposited in Gene Expression Omnibus (GSE241183).

Ethics statements

Patient consent for publication

Not applicable. Patients or the public were not involved in the design, or conduct, or reporting, or dissemination plans of our research

Ethics approval

The study was approved by the local ethics committee (Berkshire (REC 16/SC/0265) and London Bridge (REC 17/LO/0266) and conformed to the Helsinki declaration principles.

References

1. Platt L, French CE, McGowan CR, et al. Prevalence and burden of HBV co-infection among people living with HIV: A global systematic review and meta-analysis. *Journal of viral hepatitis* 2020;27(3):294-315. doi: 10.1111/jvh.13217 [published Online First: 20191222]
2. Iannacone M, Guidotti LG. Immunobiology and pathogenesis of hepatitis B virus infection. *Nature reviews Immunology* 2022;22(1):19-32. doi: 10.1038/s41577-021-00549-4 [published Online First: 20210517]
3. Boni C, Fisicaro P, Valdatta C, et al. Characterization of hepatitis B virus (HBV)-specific T-cell dysfunction in chronic HBV infection. *Journal of virology* 2007;81(8):4215-25.
4. Schurich A, Khanna P, Lopes AR, et al. Role of the coinhibitory receptor cytotoxic T lymphocyte antigen-4 on apoptosis-Prone CD8 T cells in persistent hepatitis B virus infection. *Hepatology (Baltimore, Md)* 2011;53(5):1494-503. doi: 10.1002/hep.24249 [published Online First: 2011/03/02]
5. Nebbia G, Peppia D, Schurich A, et al. Upregulation of the tim-3/galectin-9 pathway of T cell exhaustion in chronic hepatitis B virus infection. *PloS one* 2012;7(10):e47648. doi: 10.1371/journal.pone.0047648 [published Online First: 2012/11/01]
6. Rossi M, Vecchi A, Tiezzi C, et al. Phenotypic CD8 T cell profiling in chronic hepatitis B to predict HBV-specific CD8 T cell susceptibility to functional restoration in vitro. *Gut* 2023;72(11):2123-37. doi: 10.1136/gutjnl-2022-327202 [published Online First: 20230130]
7. Schurich A, Pallett LJ, Jajbhay D, et al. Distinct Metabolic Requirements of Exhausted and Functional Virus-Specific CD8 T Cells in the Same Host. *Cell reports* 2016;16(5):1243-52. doi: 10.1016/j.celrep.2016.06.078 [published Online First: 2016/07/28]

- 503 8. Le Bert N, Gill US, Hong M, et al. Effects of Hepatitis B Surface Antigen on Virus-Specific
504 and Global T Cells in Patients With Chronic Hepatitis B Virus infection.
505 *Gastroenterology* 2020;159(2):652-64. doi: 10.1053/j.gastro.2020.04.019 [published
506 Online First: 20200414]
- 507 9. Singh KP, Crane M, Audsley J, et al. HIV-hepatitis B virus coinfection: epidemiology,
508 pathogenesis, and treatment. *AIDS* 2017;31(15):2035-52. doi:
509 10.1097/QAD.0000000000001574 [published Online First: 2017/07/12]
- 510 10. Chang JJ, Sirivichayakul S, Avihingsanon A, et al. Impaired quality of the hepatitis B virus
511 (HBV)-specific T-cell response in human immunodeficiency virus type 1-HBV
512 coinfection. *Journal of virology* 2009;83(15):7649-58. doi: 10.1128/JVI.00183-09
513 [published Online First: 20090520]
- 514 11. Lascar RM, Gilson RJ, Lopes AR, et al. Reconstitution of hepatitis B virus (HBV)-specific T
515 cell responses with treatment of human immunodeficiency virus/HBV coinfection.
516 *The Journal of infectious diseases* 2003;188(12):1815-9. doi: 10.1086/379896
517 [published Online First: 20031208]
- 518 12. Chihota BV, Wandeler G, Chilengi R, et al. High Rates of Hepatitis B Virus (HBV)
519 Functional Cure Among Human Immunodeficiency Virus-HBV Coinfected Patients on
520 Antiretroviral Therapy in Zambia. *The Journal of infectious diseases* 2020;221(2):218-
521 22. doi: 10.1093/infdis/jiz450
- 522 13. Audsley J, Avihingsanon A, Littlejohn M, et al. Long-Term TDF-Inclusive ART and
523 Progressive Rates of HBsAg Loss in HIV-HBV Coinfection-Lessons for Functional HBV
524 Cure? *J Acquir Immune Defic Syndr* 2020;84(5):527-33. doi:
525 10.1097/QAI.0000000000002386
- 526 14. Sun B, da Costa KAS, Alrubayyi A, et al. HBV/HIV co-infection remodels the immune
527 landscape and Natural Killer cell ADCC functional responses. *Hepatology (Baltimore,*
528 *Md* 2024 doi: 10.1097/HEP.0000000000000877 [published Online First: 20240430]
- 529 15. Zehn D, Thimme R, Lugli E, et al. 'Stem-like' precursors are the fount to sustain persistent
530 CD8(+) T cell responses. *Nature immunology* 2022;23(6):836-47. doi:
531 10.1038/s41590-022-01219-w [published Online First: 20220527]
- 532 16. Utzschneider DT, Charmoy M, Chennupati V, et al. T Cell Factor 1-Expressing Memory-like
533 CD8(+) T Cells Sustain the Immune Response to Chronic Viral Infections. *Immunity*
534 2016;45(2):415-27. doi: 10.1016/j.immuni.2016.07.021
- 535 17. Im SJ, Hashimoto M, Gerner MY, et al. Defining CD8+ T cells that provide the proliferative
536 burst after PD-1 therapy. *Nature* 2016;537(7620):417-21. doi: 10.1038/nature19330
537 [published Online First: 20160802]
- 538 18. Thimme R, Bertoletti A, Iannacone M. Beyond exhaustion: the unique characteristics of
539 CD8(+) T cell dysfunction in chronic HBV infection. *Nature reviews Immunology*
540 2024;24(11):775-76. doi: 10.1038/s41577-024-01097-3
- 541 19. Hao Y, Hao S, Andersen-Nissen E, et al. Integrated analysis of multimodal single-cell data.
542 *Cell* 2021;184(13):3573-87 e29. doi: 10.1016/j.cell.2021.04.048 [published Online
543 First: 2021/06/02]
- 544 20. Bernstein NJ, Fong NL, Lam I, et al. Solo: Doublet Identification in Single-Cell RNA-Seq via
545 Semi-Supervised Deep Learning. *Cell Syst* 2020;11(1):95-101 e5. doi:
546 10.1016/j.cels.2020.05.010 [published Online First: 2020/06/28]
- 547 21. Xu C, Prete M, Webb S, et al. Automatic cell-type harmonization and integration across
548 Human Cell Atlas datasets. *Cell* 2023;186(26):5876-91 e20. doi:
549 10.1016/j.cell.2023.11.026

- 550 22. Fang H, Knezevic B, Burnham KL, et al. XGR software for enhanced interpretation of
551 genomic summary data, illustrated by application to immunological traits. *Genome*
552 *Med* 2016;8(1):129. doi: 10.1186/s13073-016-0384-y [published Online First:
553 20161213]
- 554 23. Dann E, Henderson NC, Teichmann SA, et al. Differential abundance testing on single-cell
555 data using k-nearest neighbor graphs. *Nature biotechnology* 2022;40(2):245-53. doi:
556 10.1038/s41587-021-01033-z [published Online First: 20210930]
- 557 24. Zheng L, Qin S, Si W, et al. Pan-cancer single-cell landscape of tumor-infiltrating T cells.
558 *Science* 2021;374(6574):abe6474. doi: 10.1126/science.abe6474 [published Online
559 First: 20211217]
- 560 25. Moinfar AA, Theis FJ. Unsupervised Deep Disentangled Representation of Single-Cell
561 Omics. *bioRxiv* 2024:2024.11.06.622266. doi: 10.1101/2024.11.06.622266
- 562 26. Alrubayyi A, Gea-Mallorqui E, Touizer E, et al. Characterization of humoral and SARS-CoV-
563 2 specific T cell responses in people living with HIV. *Nature communications*
564 2021;12(1):5839. doi: 10.1038/s41467-021-26137-7 [published Online First:
565 2021/10/07]
- 566 27. Papadakis KA, Krempski J, Reiter J, et al. Kruppel-like factor KLF10 regulates transforming
567 growth factor receptor II expression and TGF-beta signaling in CD8+ T lymphocytes.
568 *Am J Physiol Cell Physiol* 2015;308(5):C362-71. doi: 10.1152/ajpcell.00262.2014
569 [published Online First: 20141203]
- 570 28. Kumari S, Curado S, Mayya V, et al. T cell antigen receptor activation and actin
571 cytoskeleton remodeling. *Biochim Biophys Acta* 2014;1838(2):546-56. doi:
572 10.1016/j.bbamem.2013.05.004 [published Online First: 20130514]
- 573 29. Kzhyshkowska J, Gratchev A, Goerdts S. Human chitinases and chitinase-like proteins as
574 indicators for inflammation and cancer. *Biomark Insights* 2007;2:128-46. [published
575 Online First: 20070503]
- 576 30. Bourens M, Barrientos A. A CMC1-knockout reveals translation-independent control of
577 human mitochondrial complex IV biogenesis. *EMBO Rep* 2017;18(3):477-94. doi:
578 10.15252/embr.201643103 [published Online First: 20170112]
- 579 31. Guo X, Nie H, Zhang W, et al. Contrasting cytotoxic and regulatory T cell responses
580 underlying distinct clinical outcomes to anti-PD-1 plus lenvatinib therapy in cancer.
581 *Cancer Cell* 2025;43(2):248-68 e9. doi: 10.1016/j.ccell.2025.01.001 [published Online
582 First: 20250130]
- 583 32. Raju S, Xia Y, Daniel B, et al. Identification of a T-bet(hi) Quiescent Exhausted CD8 T Cell
584 Subpopulation That Can Differentiate into TIM3(+)CX3CR1(+) Effectors and Memory-
585 like Cells. *J Immunol* 2021;206(12):2924-36. doi: 10.4049/jimmunol.2001348
586 [published Online First: 20210604]
- 587 33. Khan O, Giles JR, McDonald S, et al. TOX transcriptionally and epigenetically programs
588 CD8(+) T cell exhaustion. *Nature* 2019;571(7764):211-18. doi: 10.1038/s41586-019-
589 1325-x [published Online First: 20190617]
- 590 34. Miller BC, Sen DR, Al Abosy R, et al. Subsets of exhausted CD8(+) T cells differentially
591 mediate tumor control and respond to checkpoint blockade. *Nature immunology*
592 2019;20(3):326-36. doi: 10.1038/s41590-019-0312-6 [published Online First:
593 20190218]
- 594 35. Kurtulus S, Tripathi P, Moreno-Fernandez ME, et al. Bcl-2 allows effector and memory
595 CD8+ T cells to tolerate higher expression of Bim. *J Immunol* 2011;186(10):5729-37.
596 doi: 10.4049/jimmunol.1100102 [published Online First: 20110330]

597 36. Hensel N, Gu Z, Sagar, et al. Memory-like HCV-specific CD8(+) T cells retain a molecular
598 scar after cure of chronic HCV infection. *Nature immunology* 2021;22(2):229-39. doi:
599 10.1038/s41590-020-00817-w [published Online First: 20210104]

600 37. Kefalakes H, Koh C, Sidney J, et al. Hepatitis D Virus-Specific CD8(+) T Cells Have a
601 Memory-Like Phenotype Associated With Viral Immune Escape in Patients With
602 Chronic Hepatitis D Virus Infection. *Gastroenterology* 2019;156(6):1805-19 e9. doi:
603 10.1053/j.gastro.2019.01.035 [published Online First: 20190118]

604 38. Rutishauser RL, Deguit CDT, Hiatt J, et al. TCF-1 regulates HIV-specific CD8+ T cell
605 expansion capacity. *JCI insight* 2021;6(3) doi: 10.1172/jci.insight.136648 [published
606 Online First: 20210208]

607 39. Schuch A, Salimi Alizei E, Heim K, et al. Phenotypic and functional differences of HBV
608 core-specific versus HBV polymerase-specific CD8+ T cells in chronically HBV-infected
609 patients with low viral load. *Gut* 2019;68(5):905-15. doi: 10.1136/gutjnl-2018-
610 316641 [published Online First: 20190108]

611 40. Wieland D, Kemming J, Schuch A, et al. TCF1(+) hepatitis C virus-specific CD8(+) T cells
612 are maintained after cessation of chronic antigen stimulation. *Nature*
613 *communications* 2017;8:15050. doi: 10.1038/ncomms15050 [published Online First:
614 20170503]

615 41. Chu T, Wu M, Hoellbacher B, et al. Precursors of exhausted T cells are pre-emptively
616 formed in acute infection. *Nature* 2025 doi: 10.1038/s41586-024-08451-4 [published
617 Online First: 20250108]

618 42. McManus DT, Valanparambil RM, Medina CB, et al. An early precursor CD8(+) T cell that
619 adapts to acute or chronic viral infection. *Nature* 2025 doi: 10.1038/s41586-024-
620 08562-y [published Online First: 20250108]

621 43. Heim K, Binder B, Sagar, et al. TOX defines the degree of CD8+ T cell dysfunction in
622 distinct phases of chronic HBV infection. *Gut* 2020;70(8):1550-60. doi:
623 10.1136/gutjnl-2020-322404 [published Online First: 20201023]

624 44. Cross A, Harris JM, Arbe-Barnes E, et al. Characterisation of HBV and co-infection with
625 HDV and HIV through spatial transcriptomics. *eGastroenterology* 2024;2(3) doi:
626 10.1136/egastro-2024-100067 [published Online First: 20240711]

627 45. Duhan V, Hamdan TA, Xu HC, et al. NK cell-intrinsic FcepsilonRIgamma limits CD8+ T-cell
628 expansion and thereby turns an acute into a chronic viral infection. *PLoS pathogens*
629 2019;15(6):e1007797. doi: 10.1371/journal.ppat.1007797 [published Online First:
630 2019/06/21]

631 46. Schlums H, Cichocki F, Tesi B, et al. Cytomegalovirus infection drives adaptive epigenetic
632 diversification of NK cells with altered signaling and effector function. *Immunity*
633 2015;42(3):443-56. doi: 10.1016/j.immuni.2015.02.008 [published Online First:
634 2015/03/19]

635 47. Feray C, Lopez-Labrador FX. Is PD-1 blockade a potential therapy for HBV? *JHEP Rep*
636 2019;1(3):142-44. doi: 10.1016/j.jhepr.2019.07.007 [published Online First:
637 20190828]

638 48. Gubser C, Chiu C, Lewin SR, et al. Immune checkpoint blockade in HIV. *EBioMedicine*
639 2022;76:103840. doi: 10.1016/j.ebiom.2022.103840 [published Online First:
640 20220202]

641 49. Uldrick TS, Adams SV, Fromentin R, et al. Pembrolizumab induces HIV latency reversal in
642 people living with HIV and cancer on antiretroviral therapy. *Science translational*

- 643 *medicine* 2022;14(629):eabl3836. doi: 10.1126/scitranslmed.abl3836 [published
644 Online First: 20220126]
- 645 50. Perdomo-Celis F, Passaes C, Monceaux V, et al. Reprogramming dysfunctional CD8⁺ T
646 cells to promote properties associated with natural HIV control. *The Journal of*
647 *clinical investigation* 2022;132(11) doi: 10.1172/JCI157549
- 648 51. Pena-Asensio J, Calvo-Sanchez H, Miquel J, et al. IL-15 boosts activated HBV core-specific
649 CD8⁺ progenitor cells via metabolic rebalancing in persistent HBV infection. *iScience*
650 2024;27(1):108666. doi: 10.1016/j.isci.2023.108666 [published Online First:
651 20231207]
- 652 52. Huang YJ, Ngiow SF, Baxter AE, et al. Continuous expression of TOX safeguards exhausted
653 CD8⁺ T cell epigenetic fate. *Science immunology* 2025;10(105):eado3032. doi:
654 10.1126/sciimmunol.ado3032 [published Online First: 20250307]

655 Figure Legends

656
657
658 **Figure 1. Transcriptomic profiles of CD8⁺ T cell subsets in HBV mono-infection vs. HBV/HIV co-**
659 **infection.** (A) UMAP embedding of n = 51,843 CD8⁺ T cells from n = 11 individuals (HBV n=6; HBV/
660 HIV co-infection, n=5). (B) Expression heatmap showing distinct gene expression profiles for CD8⁺ T
661 cell subsets. Genes were selected as the 5 most significant differentially expressed genes per cluster.
662 (C) Milo cell neighbourhood differential abundance plots of the significantly enriched neighbourhoods
663 between HBV mono-infection vs. HBV/HIV co-infection (FDR <0.05). (D) Volcano plot of DESeq2
664 differential gene expression analysis; significant genes (FDR <0.05 and average log2FC >|< 0.25) are
665 highlighted. The direction is in favour of HBV/HIV co-infection, for example, positive fold changes are
666 upregulated in HBV/HIV co-infection versus HBV mono-infection. (E) Bar plot of most significantly
667 enriched (FDR <0.005) reactome pathways in HBV/HIV co-infection versus HBV mono-infection. (F)
668 Differential expression analysis of DRVI derived gene programmes (denoted numerically as DRs). (G)
669 UMAP embedding showing activity of DR17. (H) Top identified genes for DR17. (I) The expression of
670 relevant genes on UMAP. (J) The activity of the Tplex score on UMAP. Abbreviations: HBV, Hepatitis B
671 Virus; HIV, Human immunodeficiency virus; FDR, false discovery rate; UMAP, uniform manifold
672 approximation and projection; DR, Dimensionality reduction.

673
674 **Figure 2. Stem-like CD8⁺ T cells are enriched in HBV/HIV co-infection.** (A) viSNE analysis
675 conducted on CD8⁺ T cells using concatenated files from HBV/HIV+ (n=20), HBV+ (n=20), and
676 HIV+ (n = 21) donors in each study group. Each point on the high-dimensional mapping represents an
677 individual cell, and colour intensity represents the expression of selected markers. (B) viSNE map of
678 FlowSOM metaclusters of CD8⁺ T cells from people with HBV/HIV, HBV, or HIV. Metaclusters are
679 colour-coded. Cell count of each FlowSOM metaclusters out of total CD8⁺ T cells (20,000
680 cells/group). Heatmap of the selected markers for CD8⁺ T cell clusters. (C) Frequency of
681 CD127⁺TCF-1⁺CD45RA⁺CCR7^{-low}CD8⁺ T cells via traditional gating in all patient groups. Summary
682 data of the proportion of CD127⁺TCF-1⁺CD45RA⁺CCR7^{-low}CD8⁺ T cells in the study groups
683 Significance determined by two-tailed Mann–Whitney U test.

Figure 3. Phenotypic characterisation of Tpex and Tex CD8⁺ T cells in peripheral blood of donors with HBV/HIV, HBV, and HIV infection. (A) Representative flow plots of gating strategy for identifying Tpex and Tex. (B) Representative flow plots of Tpex and Tex profiles identified by expression of TCF-1, CD127 and PD-1 in peripheral blood and (C) summary data from HBV/HIV+ (n = 19), HBV+ (n=20), and HIV+ (n=20) donors. Representative histogram and summary data of TOX MFI on (D) Tpex and (E) Tex CD8⁺ T cells from HBV/HIV+ (n = 19), HBV+ (n=20), and HIV+ (n=20) donors. Bar charts show the median value with interquartile range and each dot represents one donor in a group. Statistical significance was assessed by Kruskal-Wallis with Dunn's multiple comparison test.

Figure 4. Composition of HBV and HIV-specific CD8⁺ T cells in HBV/HIV, HBV, and HIV infection. Intracellular cytokine staining (ICS) was performed to examine virus-specific CD8⁺ T cells to the indicated peptide pools in HBV/HIV+ (n=20), HBV+ (n=20), and HIV+ (n = 21) donors. (A) Representative flow cytometric plots for the identification of antigen-specific CD8⁺ T cells based on double expression (IFN-γ⁺TNF-α⁺) following overnight stimulation with DMSO in media (control), CEF pool (positive control) or overlapping HBV-S, HBV-core and HIV-gag peptides. (B) Summary of aggregated CD8⁺ T-cell responses (IFN-γ⁺TNF-α⁺) against CEF, HBV-S, HBV-core or HIV-gag peptide pools from HBV/HIV+ (n=20), HBV+ (n=20), and HIV+ (n = 21) donors. (C) Proportion of detectable and non-detectable virus-specific CD8⁺ T cell responses in HBV/HIV+, HBV+, and HIV+ donors. (D) Pie charts representing the polyfunctional subsets of CEF-, HBV-S-, HBV-core- or HIV-gag-specific CD8⁺ T cell responses with IFN-γ, TNF-α and IL-2 expression, and pie arcs denoting the relative proportions of virus-specific CD8⁺ T cell response for one(red), two (blue) and three (green) cytokines. Statistical significance was assessed by Kruskal-Wallis with Dunn's multiple comparison test ($p < 0.05$).

Figure 5. Ex vivo HBV-specific CD8⁺ T cells in HBV/HIV co-infection. (A) a representative plot of HBV_{env}-specific CD8⁺ T cell identification by dextramer staining. Representative flow plot (red: HBV_{env}-specific CD8⁺ T cell; grey: corresponding global CD8⁺ T cells) and summary data of CD127/PD-1 co-expression analysis of HBV_{env}-specific CD8⁺ T cells derived from individuals with HBV/HIV (n = 6). (B) Representative histogram and gating of TCF-1 expression on HBV_{env}-specific CD8⁺ T and global CD8⁺ T cells and summary data of TCF-1 expression on HBV_{env}-specific CD8⁺ T with respect to CD127/PD-1 subsets. (C) Representative histogram and gating of BCL-2 expression on HBV_{env}-specific CD8⁺ T and global CD8⁺ T cells and summary data of BCL-2 expression on HBV_{env}-specific CD8⁺ T with respect to CD127/PD-1 subsets. Representative histograms of the individual markers are depicted (grey: corresponding global CD8⁺ T cells and red: HBV epitope-specific CD8⁺ T cells). Bar charts show the median value with interquartile range. Statistics were performed using a two-tailed Wilcoxon matched-pairs signed-rank test ($p < 0.05$).

725

726 **Figure 6. Virological parameters and correlation analysis.** (A) HBsAg level quantification (log
727 HBsAg, IU/ml) from individuals with HBV/HIV and HBV. Data shown as scatter plots with the group
728 median and interquartile range indicated. (B) Proportion of HBV/HIV+ or HBV+ donors within a given
729 range of HBsAg level (IU/ml). (C) Correlogram of individuals with HBV/HIV and HBV utilised for
730 phenotypic and functional characterisation. Spearman r values shown from red (−1) to blue (1) with r
731 values indicated by colour. Spearman r value shown. *p<0.05, **p<0.01, and ***p<0.001.
732

Figure 1

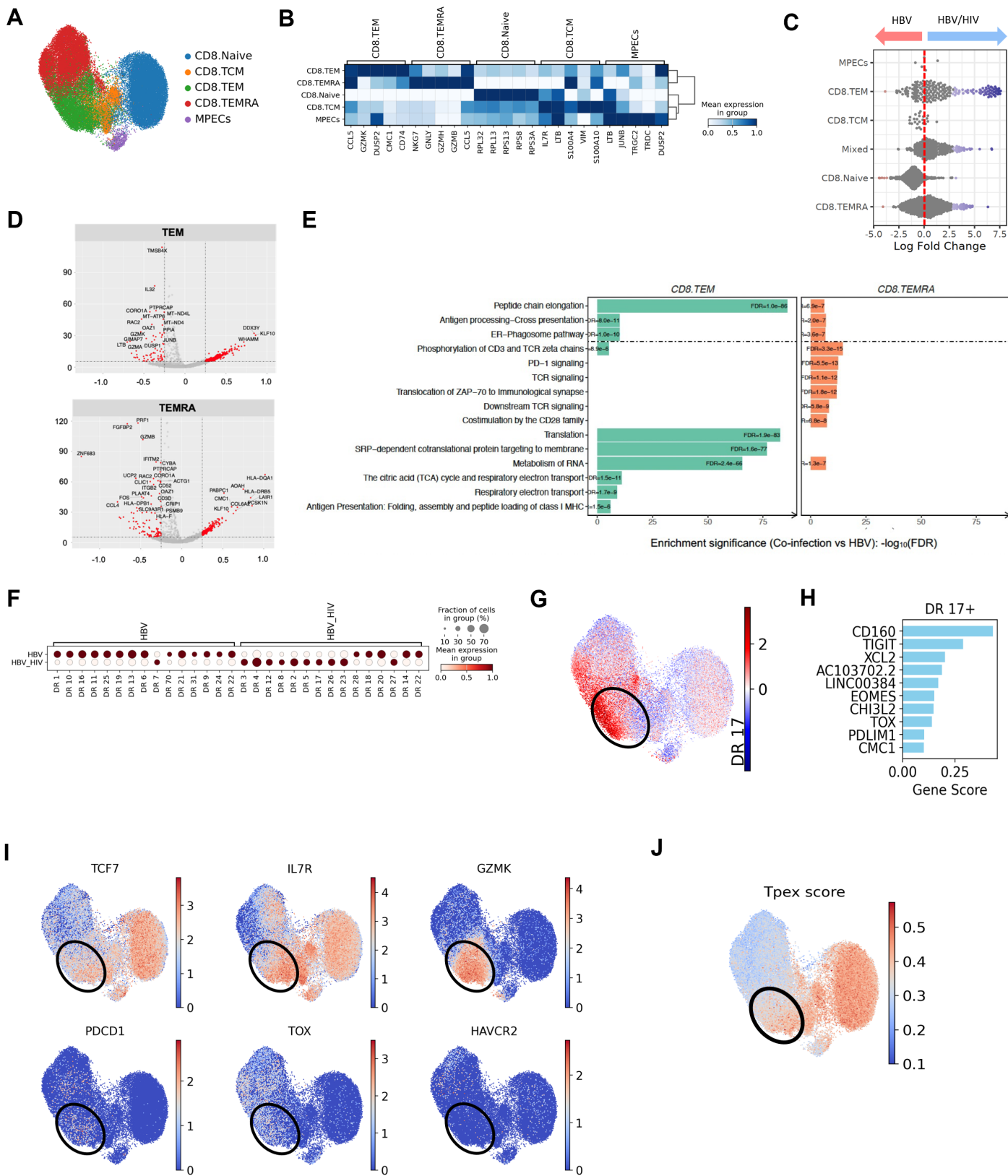
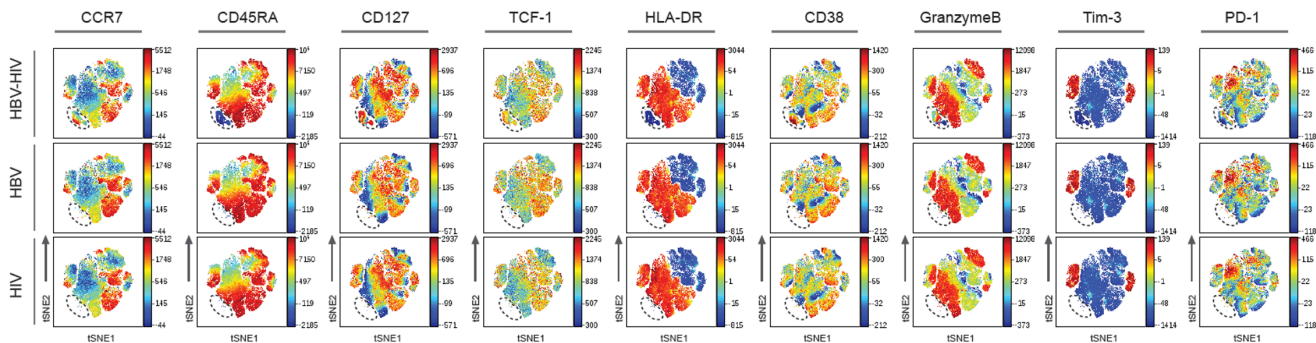
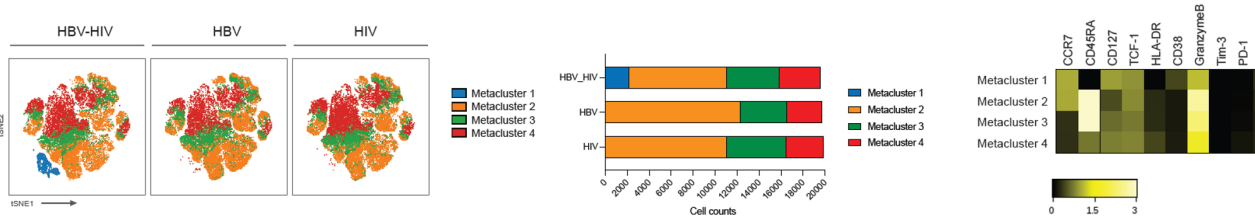


Figure 2

A



B



C

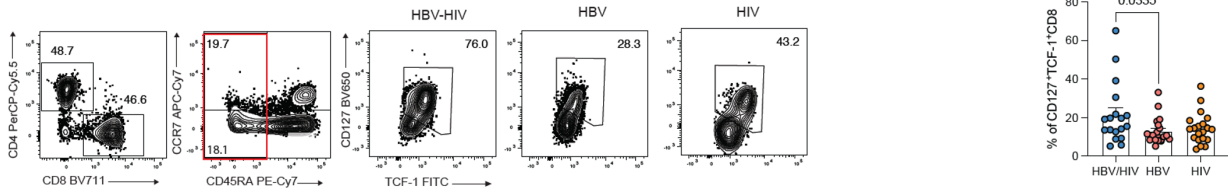


Figure 3

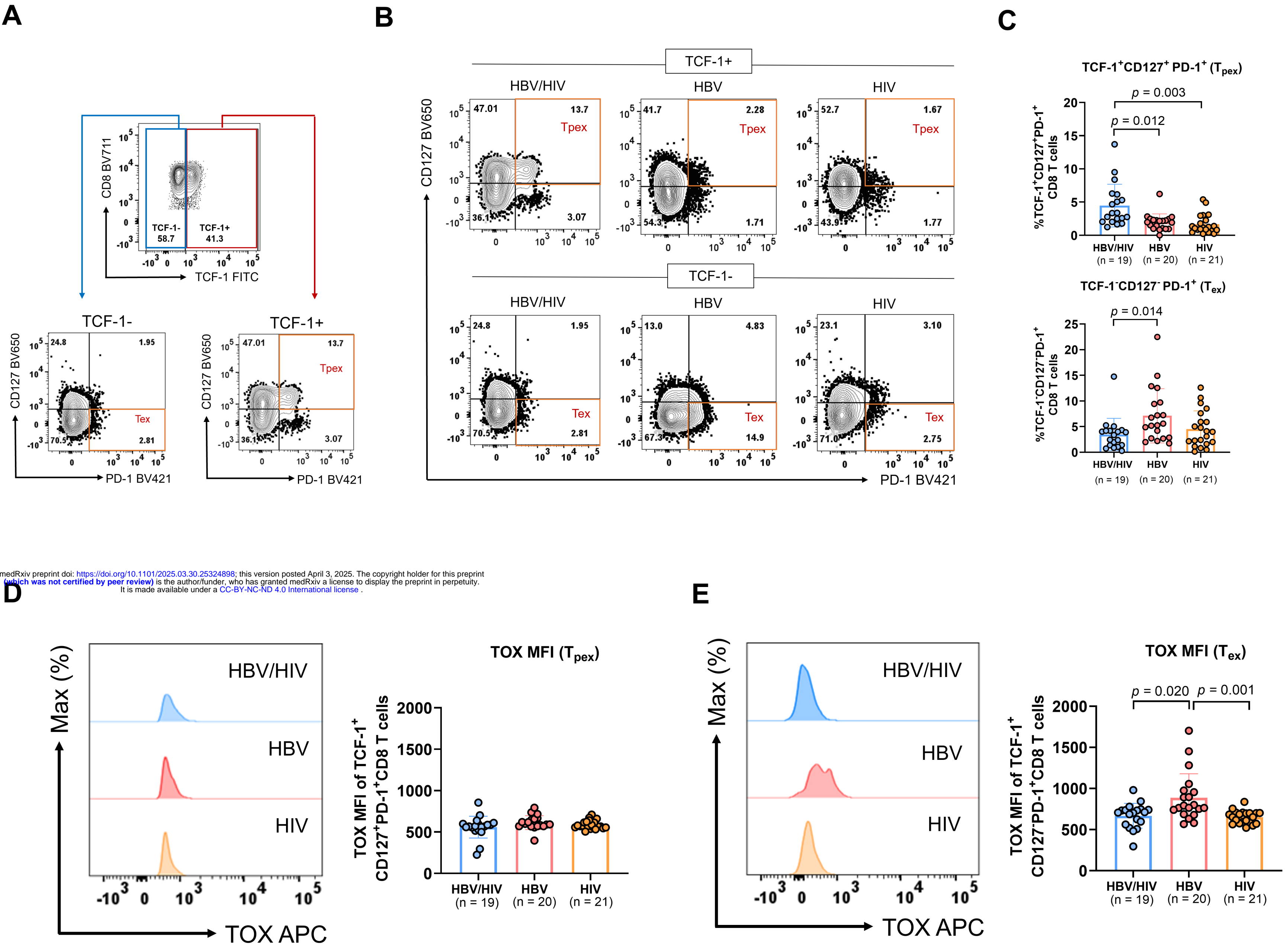


Figure 4

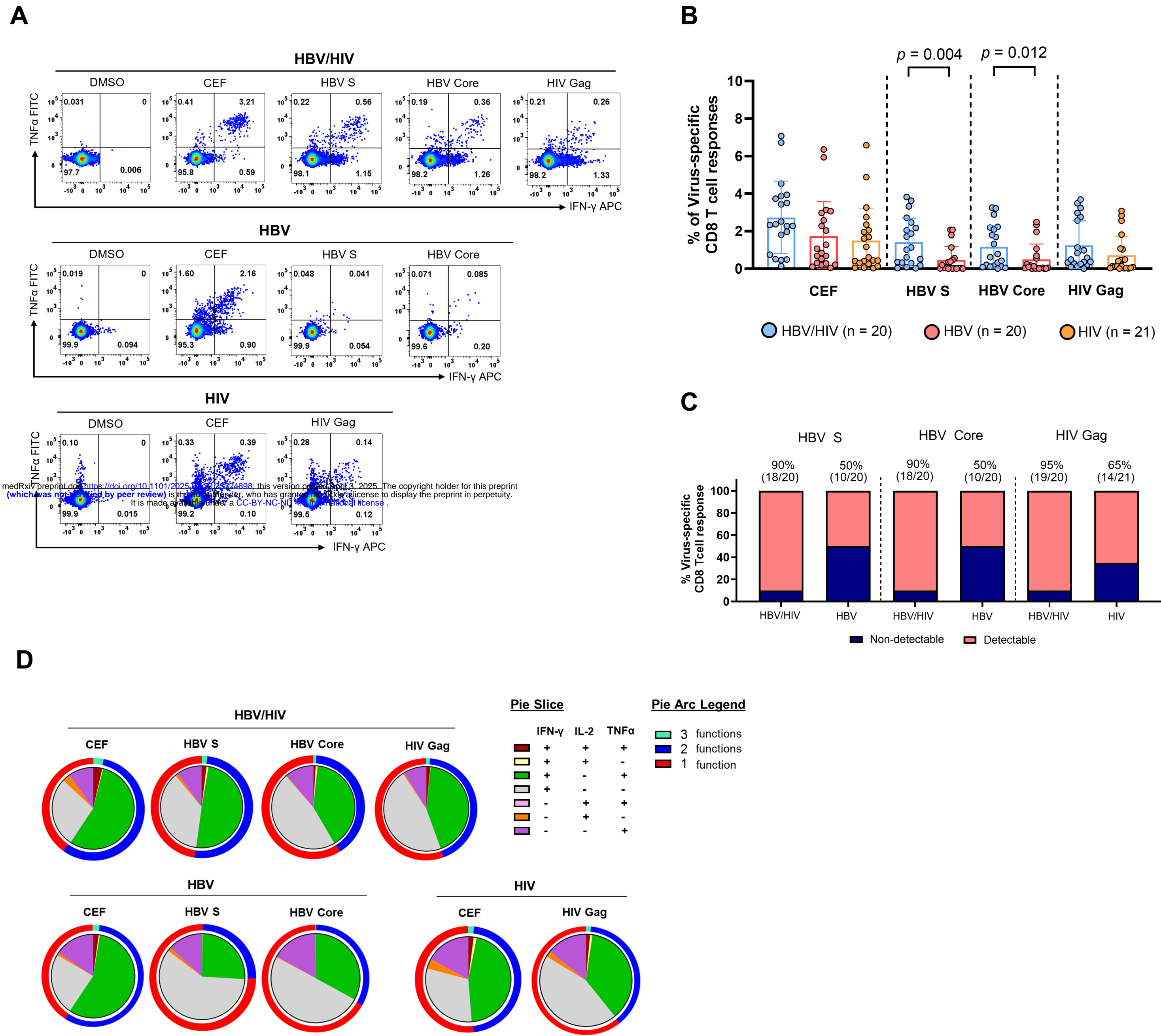
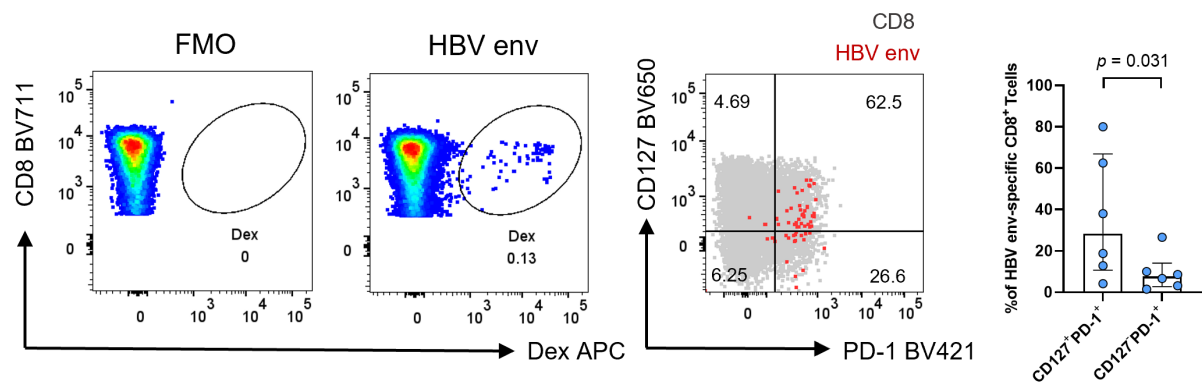
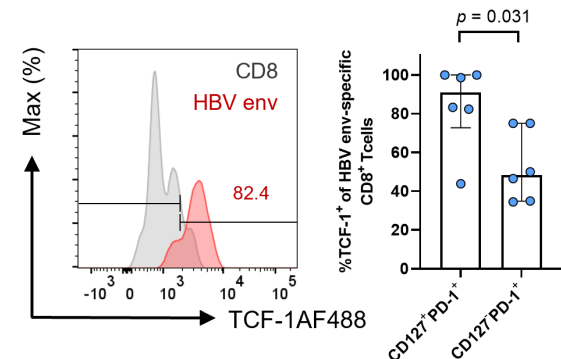


Figure 5

A



B



C

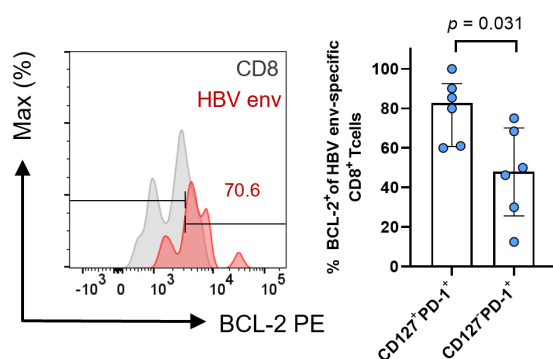
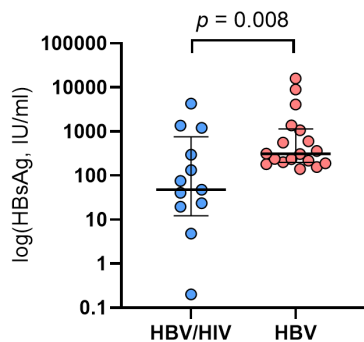


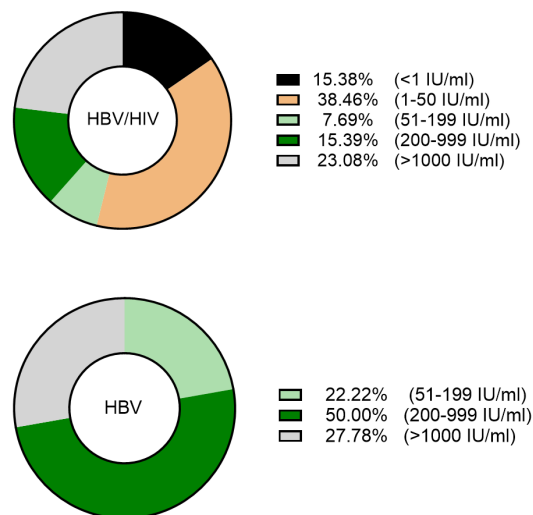
Figure 6

A



B

HBsAg range



C

